

Harmonic map analysis of $SU(N)$ gravitating Skyrmions

Yves Brihaye *

Faculté des Sciences, Université de Mons, 7000 Mons, Belgium

Betti Hartmann †

*School of Engineering and Sciences,
International University Bremen (IUB), 28275 Bremen, Germany*

Theodora Ioannidou ‡

Institute of Mathematics, University of Kent, Canterbury CT2 7NF, UK

Wojtek Zakrzewski§

*Department of Mathematical Sciences,
University of Durham, Durham DH1 3LE, U.K.*

(Dated: January 7, 2019)

Abstract

In this paper the $SU(N)$ Einstein-Skyrme system is considered. We express the chiral field (which is not a simple embedding of the $SU(2)$ one) in terms of harmonic maps. In this way, $SU(N)$ spherical symmetric equations can be obtained easily for any N and the gravitating skyrmion solutions of these equations can be studied. In particular, the $SU(3)$ case is considered in detail and three different types of gravitating skyrmions with topological charge 4, 2 and 0, respectively, are constructed numerically. Note that the configurations with topological charge 0 correspond to mixtures of skyrmions and antiskyrmions.

PACS numbers: 04.20.Jb, 04.40.Nr, 12.39.Dc

* yves.brihaye@umh.ac.be

† b.hartmann@iu-bremen.de

‡ T.Ioannidou@ukc.ac.uk

§ W.J.Zakrzewski@durham.ac.uk

I. INTRODUCTION

Nonlinear field theories coupled to gravity have received a lot of interest in the past decade. It has been discovered that gravitational interaction may lead to genuinely nonperturbative phenomena like gravitationally bound configurations of nonabelian fields, while the study of black hole solutions in various models revealed the possibility of nonlinear hair on black holes [1] which questioned the validity of the unqualified no-hair conjecture.

One of the candidates of such investigations is the Einstein-Skyrme model which can e.g. describe the interaction between a baryon and a black hole (a configuration which might have been produced in the very early universe). So far, most of the studies have concentrated on the $SU(2)$ Einstein-Skyrme model [2, 3, 4]. In particular, in [2] it has been shown that the Schwarzschild black hole can support chiral (“Skyrme”) hair and it has been argued that such configurations might be stable. The presence of the horizon in the core of the skyrmion unwinds the skyrmion, leaving fractional baryon charge outside the horizon. More systematic investigations of the model were undertaken in [3] by solving numerically the static spherically symmetric Einstein-Skyrme equations. Globally regular solutions with baryon number one [4] and black holes with chiral hair were found and their stability properties were studied in detail [3, 4].

The first examples of nonembedded solutions for a higher group, namely the $SU(3)$ group, were the $SO(3)$ solitons with even topological charge. The lowest energy solution corresponds to a bound state of two gravitating skyrmions [5]. Specifically, it was found that the two branches of these regular solutions exist, which merge at a critical value of the gravitational coupling.

In this paper we consider particle-like solutions of the $SU(N)$ Einstein-Skyrme model (for $N \geq 2$). In particular, we study the deformation of the multiskyrmion configurations [6] (derived using the harmonic map ansatz) when gravity is introduced. Note that the use of harmonic maps for gravitating skyrmions can be traced to [7]. New types of solutions are found, which correspond to skyrmion-antiskyrmion configurations and have topological charge 0. Like the non-gravitating skyrmion-antiskyrmions, these configurations are also saddle points of the energy functional and thus are likely to be unstable.

Our paper is organised as follows: in Section II, we present the $SU(N)$ Einstein-Skyrme model, while in Section III we give the harmonic map ansatz. In Section IV, we present the

spherically symmetric equations of motion and in Section V we discuss our numerical results for the $SU(3)$ case. In this latter section, we also point out that we recover the already known solutions for the topological charge 4 and 2 [5], but also derive new solutions describing the gravitating skyrmion-antiskyrmions with the topological charge 0. Our conclusions are summarised in Section VI.

II. THE $SU(N)$ EINSTEIN-SKYRME MODEL

The $SU(N)$ Einstein-Skyrme action reads:

$$S = \int \left[\frac{R}{16\pi G} - \frac{1}{2} \text{tr}(K_\mu K^\mu) - \frac{1}{16} \text{tr}([K_\mu, K_\nu][K^\mu, K^\nu]) \right] \sqrt{-g} d^4x \quad (1)$$

where $K_\mu = \partial_\mu U U^{-1}$ for $\mu = 0, 1, 2, 3$ and $U(x^\mu) \in SU(N)$ is the matter field, g denotes the determinant of the metric and G represents Newton's constant. In order for the finite-energy configurations to exist the Skyrme field has to go to a constant matrix at spatial infinity: $U \rightarrow I$ as $|x^\mu| \rightarrow \infty$.

To derive the classical equations of motion of our system we perform the variation of the action (1) with respect to the metric and the Skyrme field. The variation with respect to the metric $g^{\mu\nu}$ gives the Einstein equations:

$$R_{\mu\nu} - \frac{1}{2} g_{\mu\nu} R = 8\pi G T_{\mu\nu}, \quad (2)$$

where $R_{\mu\nu}$ denotes the Ricci tensor and the stress-energy tensor $T_{\mu\nu} = g_{\mu\nu} \mathcal{L} - 2 \frac{\partial \mathcal{L}}{\partial g^{\mu\nu}}$ is given by:

$$T_{\mu\nu} = \text{tr} \left(K_\mu K_\nu - \frac{1}{2} g_{\mu\nu} K_\alpha K^\alpha \right) + \frac{1}{4} \text{tr} \left(g^{\alpha\beta} [K_\mu, K_\alpha] [K_\nu, K_\beta] - \frac{1}{4} g_{\mu\nu} [K_\alpha, K_\beta] [K^\alpha, K^\beta] \right). \quad (3)$$

The variation of the action with respect to the matter fields leads to the Euler-Lagrange equations which we will discuss in the next section.

The Einstein-Skyrme system has a topological current which is covariantly conserved, yielding the topological charge [8]:

$$B = \int \sqrt{-g} B^0 d^3x, \quad (4)$$

where

$$B^\mu = -\frac{1}{24\pi^2 \sqrt{-g}} \varepsilon^{\mu\nu\alpha\beta} \text{tr}(K_\nu K_\alpha K_\beta) \quad (5)$$

and $\varepsilon^{\mu\nu\alpha\beta}$ is the (constant) fully antisymmetric tensor.

In what follows we will concentrate our attention on studying the static Einstein-Skyrme equations and we are going to construct their static spherically symmetric solutions by using harmonic maps for the Skyrme field.

III. HARMONIC MAP ANSATZ

The starting point of our investigation is the introduction of the coordinates r, z, \bar{z} on \mathbb{R}^3 . In terms of the usual spherical coordinates r, θ, ϕ the Riemann sphere variable z is given by: $z = e^{i\phi} \tan(\theta/2)$ and \bar{z} is the complex conjugate of z . In this system of coordinates the Schwarzschild-like (spherically symmetric) metric reads:

$$ds^2 = -A^2(r)C(r) dt^2 + \frac{1}{C(r)} dr^2 + \frac{4r^2}{(1 + |z|^2)^2} dzd\bar{z}, \quad C(r) = 1 - \frac{2m(r)}{r}, \quad (6)$$

where $m(r)$ is the mass function. For this metric the square-root of the determinant takes the simple form:

$$\sqrt{-g} = iA(r) \frac{2r^2}{(1 + |z|^2)^2}. \quad (7)$$

After substituting the metric (6), the action (1) becomes:

$$S = \int \left[\frac{R}{16\pi G} + \text{tr} \left(-\frac{1}{2} C K_r^2 - \frac{(1 + |z|^2)^2}{2r^2} |K_z|^2 + \frac{1}{32} \frac{(1 + |z|^2)^4}{r^4} [K_z, K_{\bar{z}}]^2 - \frac{1}{8} \frac{(1 + |z|^2)^2}{r^2} C \left| [K_r, K_z] \right|^2 \right) \right] \sqrt{-g} dt dr dzd\bar{z} \quad (8)$$

while the baryon number is equal to

$$B = -\frac{1}{8\pi^2} \int \text{tr} (K_r [K_z, K_{\bar{z}}]) dr dz d\bar{z}. \quad (9)$$

In addition, the Einstein equations (2) take the form:

$$\begin{aligned} \frac{2}{r^2} m' &= 8\pi G T_0^0 \\ \frac{2}{r} \frac{A'}{A} C &= 8\pi G (T_0^0 - T_r^r) \end{aligned} \quad (10)$$

where the prime denotes the derivative with respect to r and

$$\begin{aligned} T_0^0 &= -\frac{C}{2} \text{tr} (K_r^2) - \frac{(1 + |z|^2)^2}{2r^2} \text{tr} (|K_z|^2) - \frac{1}{8} \frac{C(1 + |z|^2)}{r^2} \text{tr} \left(\left| [K_r, K_z] \right|^2 \right) \\ &\quad - \frac{1}{32} \frac{(1 + |z|^2)^4}{r^4} \text{tr} ([K_z, K_{\bar{z}}]^2), \end{aligned} \quad (11)$$

$$T_0^0 - T_r^r = -C \text{tr} (K_r^2) - \frac{1}{4} \frac{C(1 + |z|^2)^2}{r^2} \text{tr} \left(\left| [K_r, K_z] \right|^2 \right). \quad (12)$$

Following [6] the application of the harmonic map ansatz to describe the matter fields, corresponds to setting:

$$\begin{aligned}
U &= \exp \left\{ 2i \sum_{i=0}^{N-2} g_i \left(P_i - \frac{I}{N} \right) \right\} \\
&= e^{-2ig_0/N} (1 + A_0 P_0) e^{-2ig_1/N} (1 + A_1 P_1) \dots e^{-2ig_{N-2}/N} (1 + A_{N-1} P_{N-2}) \quad (13)
\end{aligned}$$

where $g_k = g_k(r)$ for $k = 0, \dots, N-2$ are the profile functions which depend only on r . Moreover, we define also $A_k = e^{2ig_k} - 1$. The boundary value $U \rightarrow I$ at $r \rightarrow \infty$ (needed for finiteness of the action) imposes the requirement that $g_i(\infty) = 0$.

Here P_k form a set of projectors based on the maps $S^2 \rightarrow CP^{N-1}$ which are constructed as follows [9]: write each projector P as

$$P(V) = \frac{V \otimes V^\dagger}{|V|^2}, \quad (14)$$

where V is a N -component complex vector of two variables z and \bar{z} . The first projector is obtained by taking $V = f(z)$ (i.e. an analytic vector of z), while the other projectors are given in terms of new vectors V which are obtained from the original V by differentiation and Gramm-Schmidt orthogonalisation. If we define an operator P_+ by its action on any vector $v \in \mathbb{C}^N$ [10] as

$$P_+ v = \partial_z v - v \frac{v^\dagger \partial_z v}{|v|^2}, \quad (15)$$

then the vectors $V_k = P_+^k v$ can be defined by induction: $P_+^k v = P_+(P_+^{k-1} v)$.

Therefore, in general, we can consider projectors P_k of the form (14) corresponding to the family of vectors $V \equiv V_k = P_+^k f$ (for $f = f(z)$) as

$$P_k = P(P_+^k f), \quad k = 0, \dots, N-1, \quad (16)$$

where, due to the orthogonality of the projectors, we have $\sum_{k=0}^{N-1} P_k = 1$. This follows from the following properties of vectors $P_+^k f$ (which hold when f is holomorphic):

$$\begin{aligned}
(P_+^k f)^\dagger P_+^l f &= 0 \quad \text{for } k \neq l, \\
\partial_{\bar{z}} (P_+^k f) &= -P_+^{k-1} f \frac{|P_+^k f|^2}{|P_+^{k-1} f|^2}, \quad \partial_z \left(\frac{P_+^{k-1} f}{|P_+^{k-1} f|^2} \right) = \frac{P_+^k f}{|P_+^{k-1} f|^2}. \quad (17)
\end{aligned}$$

Note that, for $SU(N)$, the last projector in the sequence, P_{N-1} , corresponds to an anti-analytic vector (i.e. a function of \bar{z}). Moreover, we can always express one projector as a sum of the others.

It was shown in [6] (for the non-gravitating spherical symmetric skyrmions) that the chiral field (13) is an exact solution of the corresponding equations when

$$f = (f_0, \dots, f_j, \dots, f_{N-1})^t \quad \text{where} \quad f_j = z^j \sqrt{\binom{N-1}{j}} \quad (18)$$

and $\binom{N-1}{j}$ denote the binomial coefficients. In what follows we apply the same ansatz to obtain the corresponding gravitating skyrmions for the simplest cases of $SU(2)$ and $SU(3)$. These cases will clarify the expressions for the general $SU(N)$ case.

IV. SPHERICAL SYMMETRIC EQUATIONS OF MOTION

In the case of spherical symmetry, the action (1) using (13) takes the form

$$S = 2\pi \int \left\{ \frac{RAr^2}{8\pi G} - \frac{4}{N} r^2 CA \left(\sum_{i=0}^{N-2} g'_i \right)^2 + 4r^2 CA \sum_{i=0}^{N-2} g_i'^2 + 2A \sum_{k=1}^{N-1} D_k \right. \\ \left. + \frac{A}{4r^2} \left[D_1^2 + \sum_{i=1}^{N-2} (D_i - D_{i+1})^2 + D_{N-1}^2 \right] + 2CA \sum_{k=1}^{N-1} D_k (g'_k - g'_{k-1})^2 \right\} dr dt, \quad (19)$$

where $D_k = 2k(N-k) \sin^2(g_k - g_{k-1})$. The matter equations are obtained from the variation of this action with respect to the matter field. We will present these equations when considering the specific cases of $SU(2)$ and $SU(3)$.

In addition, the Einstein equations (10) take the form:

$$\frac{2}{r^2} m' = 16\pi G \left[-\frac{C}{N} \left(\sum_{i=0}^{N-2} g'_i \right)^2 + C \sum_{i=0}^{N-2} g_i'^2 + \frac{1}{2r^2} \sum_{k=1}^{N-1} D_k + \frac{C}{2r^2} \sum_{k=1}^{N-1} D_k (g'_k - g'_{k-1})^2 \right. \\ \left. + \frac{1}{16r^4} \left(D_1^2 + \sum_{i=1}^{N-2} (D_i - D_{i+1})^2 + D_{N-1}^2 \right) \right] \quad (20)$$

$$\frac{2}{r} \frac{A'}{A} C = 16\pi G \left[-\frac{2C}{N} \left(\sum_{i=0}^{N-2} g'_i \right)^2 + 2C \sum_{i=0}^{N-2} g_i'^2 + C \frac{1}{r^2} \sum_{k=1}^{N-1} D_k (g'_k - g'_{k-1})^2 \right]. \quad (21)$$

For simplicity, we set $F_k = g_k - g_{k+1}$ for $k = 0, \dots, N-2$ with $F_{N-2} = g_{N-2}$. Then, the topological charge (9) simplifies to

$$B = \frac{1}{\pi} \sum_{i=0}^{N-2} (i+1)(N-i-1) \left(F_i - \frac{\sin 2F_i}{2} \right) \Big|_0^\infty. \quad (22)$$

Since $F_i(\infty) = 0$ the only contributions to the topological charge come from $F_i(0)$.

The main symmetry of our expressions is the symmetry under the independent interchanges

$$F_k \leftrightarrow F_{N-k-2}, \quad k = 0, \dots, N-2 \quad (23)$$

which follows from the fact that the D_k terms in (19) are symmetric under the interchange $D_k \leftrightarrow D_{N-k}$ when $F_{k-1} \leftrightarrow F_{N-k-1}$. At the same time, all the other terms in (19) exhibit this symmetry since they are combinations of F_i and their derivatives.

A. $SU(2)$

For $N = 2$ there is only one profile function, $F_0(r)$, and (19) simplifies to

$$S = 2\pi \int \left\{ \frac{RAr^2}{8\pi G} + 2r^2 C A F_0'^2 + 4A \sin^2 F_0 + 2A \frac{\sin^4 F_0}{r^2} + 4C A \sin^2 F_0 F_0'^2 \right\} dr dt, \quad (24)$$

while its variation with respect to the profile function gives us the matter equation:

$$\left[C A r^2 F_0' \left(1 + \frac{2 \sin^2 F_0}{r^2} \right) \right]' - A \sin 2F_0 \left(1 + \frac{\sin^2 F_0}{r^2} + C F_0'^2 \right) = 0. \quad (25)$$

The Einstein equations (21) now take the form:

$$\frac{2}{r^2} m' = 8\pi G \left[C F_0'^2 + \frac{2 \sin^2 F_0}{r^2} (1 + C F_0'^2) + \frac{\sin^4 F_0}{r^4} \right], \quad (26)$$

$$\frac{2}{r} \frac{A'}{A} = 16\pi G F_0'^2 \left(1 + 2C \frac{\sin^2 F_0}{r^2} \right). \quad (27)$$

There is only one solution with the boundary condition $F_0(0) = \pi$. This solution has topological charge $B = 1$ (see (22)) and has previously been studied in great detail in [3, 4].

Therefore we will not repeat these calculations here.

B. $SU(3)$

For $N = 3$ there are two profile functions, $F_0(r)$, $F_1(r)$, and (19) becomes

$$S = 2\pi \int \left\{ \frac{RAr^2}{8\pi G} + \frac{8}{3} r^2 C A (F_0'^2 + F_1'^2 + F_0' F_1') + 8A (\sin^2 F_0 + \sin^2 F_1) + \frac{8A}{r^2} (\sin^4 F_0 - \sin^2 F_0 \sin^2 F_1 + \sin^4 F_1) + 8C A (\sin^2 F_0 F_0'^2 + \sin^2 F_1 F_1'^2) \right\} dr dt \quad (28)$$

The corresponding equations for F_0 and F_1 are now given by:

$$\left[r^2 C A F_0' \left(\frac{2}{3} + \frac{2 \sin^2 F_0}{r^2} \right) + \frac{r^2}{3} C A F_1' \right]' - A \sin 2F_0 \left(1 + \frac{2 \sin^2 F_0 - \sin^2 F_1}{r^2} + C F_0'^2 \right) = 0, \quad (29)$$

$$\left[r^2 C A F_1' \left(\frac{2}{3} + \frac{2 \sin^2 F_1}{r^2} \right) + \frac{r^2}{3} C A F_0' \right]' - A \sin 2F_1 \left(1 + \frac{2 \sin^2 F_1 - \sin^2 F_0}{r^2} + C F_1'^2 \right) = 0 . \quad (30)$$

Note that the above equations are symmetric under the simultaneous interchange $F_0 \rightarrow F_1$ and $F_1 \rightarrow F_0$.

Finally, the Einstein equations (10) take the form:

$$\frac{2}{r^2} m' = 32\pi G \left[\frac{C}{3} (F_0'^2 + F_0' F_1' + F_1'^2) + \frac{1}{r^2} (\sin^2 F_0 + \sin^2 F_1) + \frac{C}{r^2} (\sin^2 F_0 F_0'^2 + \sin^2 F_1 F_1'^2) + \frac{1}{r^4} (\sin^4 F_0 - \sin^2 F_0 \sin^2 F_1 + \sin^2 F_1) \right] , \quad (31)$$

$$\frac{2}{r} \frac{A'}{A} = 64\pi G \left[\frac{1}{3} (F_0'^2 + F_0' F_1' + F_1'^2) + \frac{\sin^2 F_0}{r^2} F_0'^2 + \frac{\sin^2 F_1}{r^2} F_1'^2 \right] . \quad (32)$$

The set of equations (29)-(32) can only be solved numerically when the right boundary conditions have been imposed. Similarly to the flat case [6], we see that there exist three types of gravitating multiskyrmions, which we will discuss in detail in the following section.

V. NUMERICAL SIMULATIONS

To solve the equations (29)-(32) numerically, we have adopted the numerical routine described in [11]. For convenience, we define $\alpha^2 = 16\pi G$ so that the flat limit with $C(r) = A(r) = 1$ corresponds to $\alpha = 0$.

A. Boundary conditions

As will be discussed in more detail in the following, three kinds of regular finite-energy solutions exist with the following boundary conditions:

$$\begin{aligned} \text{(I)} \quad & F_0(0) = \pi, & F_1(0) = \pi, \\ \text{(II)} \quad & F_0(0) = \pi, & F_1(0) = -\pi, \\ \text{(III)} \quad & F_0(0) = \pi, & F_1(0) = 0, \end{aligned} \quad (33)$$

and for all these cases

$$\text{(I) / (II) / (III)} : F_0(\infty) = 0 \quad , \quad F_1(\infty) = 0 . \quad (34)$$

Furthermore, we have the two supplementary conditions for the metric functions:

$$\text{(I) / (II) / (III)} : m(0) = 0 \quad , \quad A(\infty) = 1 . \quad (35)$$

The condition that $m(r)$ vanishes at the origin $r = 0$ is due to the requirement of regularity, while the second condition for $A(r)$ results from the requirement of asymptotic flatness. The energy E of the gravitating skyrmions can then be determined from the “mass function” $m(r)$ at infinity:

$$E = \frac{4m(\infty)}{3\pi\alpha^2} . \quad (36)$$

With this normalisation, the values of E can be compared to those of the flat limit [6].

Our numerical analysis demonstrates that the three solutions are indeed continuously deformed by gravity ($\alpha > 0$). Next we discuss our numerical results for each set of conditions given in (33).

B. Case I

This case corresponds to choosing $F_0(r) = F_1(r)$. Apart from a trivial rescaling of the coupling constants [5], the equations for the matter and metric functions are equal to those of the gravitating $SU(2)$ skyrmion, which were studied in great detail in [3, 4]. However, for completeness, we again present the main features of these solutions.

The non-gravitating solution has energy $E \approx 4.928 = 4 \times 1.232$, i.e. four times the energy of the $SU(2)$ one-skyrmion. Due to the boundary conditions $F_0(0) = F_1(0) = \pi$ the topological charge is four (see (22)). The non-gravitating solution can thus be interpreted as four noninteracting skyrmions placed on top of each other in such a way that the baryon (energy) density is spherically symmetric.

As for the asymptotic behaviour, we notice that the chiral field is of the form

$$\begin{aligned} F_0(r) = F_1(r) &\approx \pi - B_I r & \text{for } 0 \leq r \ll 1 , \\ F_0(r) = F_1(r) &\approx \frac{\tilde{B}_I}{r^2} & \text{for } r \gg 1 , \end{aligned} \quad (37)$$

where B_I, \tilde{B}_I are (shooting) parameters depending on α which have to be determined numerically.

Solving numerically the system (29)-(32) for $\alpha > 0$ we find that the flat solution is gradually deformed by gravity, forming a branch of gravitating skyrmions. In particular, the function $C(r)$ develops a local minimum at some intermediate radius : $r = r_m(\alpha)$, while the function $A(r)$ has a minimum $A_{min} = A(0)$ at the origin and then increases monotonically.

However, the profile functions of the Skyrme field deviate only slightly from the corresponding ones in the flat limit. Moreover, as α increases, the respective minimal values of the metric functions $C(r)$, $A(r)$, i.e. $C_m = C(r_m)$ and $A_0 = A(0)$ both decrease and so does the corresponding energy E . This latter decrease is, of course, expected since gravity tends to lower the mass of a solution. The four skyrmions can thus be seen as “gravitationally bound”. This is illustrated in Fig. 1 (solid lines). Note that this branch of gravitating skyrmions does not exist for arbitrarily large values of α , but only up to some critical value α_{cr} : $\alpha \leq \alpha_{cr} \approx 0.142087$ (as shown in Fig. 1). Also the quantities A_0 , C_m as functions of α remain finite with

$$E(\alpha = \alpha_{cr}) \approx 4.20, \quad A_0(\alpha = \alpha_{cr}) \approx 0.437, \quad C_m(\alpha = \alpha_{cr}) \approx 0.584. \quad (38)$$

Our numerical analysis, however, strongly suggests that a second branch of solutions exists in the interval $[0, \alpha_{cr}]$. For a given α , the solution of the second branch has a higher energy than the one on the main branch while A_0 , C_m have lower values as shown in Fig. 1 (dotted lines). For $\alpha \rightarrow \alpha_{cr}$ both branches go to the same solution but the solution of the second branch becomes more and more peaked around the origin (i.e. the slope $F'(0)$ tends to infinity). As a consequence (in this limit) the energy on the upper branch diverges as $\alpha \rightarrow 0$, but the product αE remains finite (≈ 0.124). This solution, rescaled according to $x \rightarrow \frac{x}{\alpha}$ stays regular in the $\alpha \rightarrow 0$ limit and converges to the sphaleron solution of the Einstein-Yang-Mills system [5, 12]. Note that the metric functions remain finite and are strictly positive. Therefore, no black hole solution is generated by the solutions of the equations under consideration, in contrast to e.g. the Einstein-Yang-Mills-Higgs equations [13].

C. Case II

By choosing $F_0(r) = -F_1(r)$ with the boundary conditions $F_0(0) = -F_1(0) = \pi$, the nongravitating solution is topologically trivial since the topological charge is zero. However, this configuration is not the vacuum solution, but consists of two skyrmions and two antiskyrmions. Note that these solutions were not studied previously in [5].

The regularity of the solutions at the origin requires that $F'_0(0) = 0$ which has been checked by us numerically to hold within a very high level of accuracy. The flat solution

($\alpha = 0$) has energy $E \approx 3.861$ and was discussed in detail in [6].

It is worth noticing that the asymptotic behaviour of the Skyrme function $F_0(r)$ differs drastically from the one of case I:

$$\begin{aligned} F_0(r) &\approx \pi - B_{II}r^2 & \text{for } 0 \leq r \ll 1 \text{ ,} \\ F_0(r) &\approx \frac{\tilde{B}_{II}}{r^3} & \text{for } r \gg 1 \text{ .} \end{aligned} \quad (39)$$

For $\alpha > 0$ the pattern of the solutions is very similar to the one occurring in case I. The critical value of α is larger than in I with $\alpha_{cr} \approx 0.1834$. This is related to the fact that the solutions of case I are heavier (compare the flat limit energies) and thus exist for a smaller interval of the gravitational coupling. We note that

$$E(\alpha = \alpha_{cr}) \approx 3.377, \quad A_0(\alpha = \alpha_{cr}) \approx 0.517, \quad C_m(\alpha = \alpha_{cr}) \approx 0.614. \quad (40)$$

The occurrence of two branches is illustrated in Fig. 2, where the energy E of the solution and the quantities C_m, A_0 are plotted as a function of α .

In the limit $\alpha \rightarrow 0$ on the upper branch, the solution again converges to the SU(3) Einstein-Yang-Mills sphaleron solution constructed first in [12]. When solving the equations numerically, the main feature of the present charge 0 solution resides in the fact that the derivative of the chiral function $F_0(r)$, $F'_0(r)$, vanishes at the origin $r = 0$ and thus the ‘‘shooting’’ parameter is the second derivative $F''_0(r)|_{r=0}$. This renders the numerical analysis more involved than in the first case. The solutions’ profiles corresponding to the lower and upper branches are shown in Fig. 3 for $\alpha = 0.17$. In this figure, a logarithmic scale is used in order to reveal the completely different behaviour of $F'_0(r)$ as $r \rightarrow 0$. The value $F''_0(r)|_{r=0}$ for the solution on the upper branch is several orders of magnitude larger than its counterpart on the lower branch. More generally, we noticed that the shooting parameter $F''_0(r)|_{r=0}$ varies surprisingly strongly with α and increases considerably when α increases (resp. decreases) on the lower (resp. upper) branch.

D. Case III

In this case we choose $F_0(0) = \pi$, $F_1(0) = 0$ and $F_1(r)$ goes from zero to zero developing one node at some finite value of r . Due to the boundary conditions, these solutions have

topological charge 2 and are the gravitating $SO(3)$ embedded solutions discussed in [5]. The flat limit ($\alpha = 0$) solutions have been studied in [14]. Again, for completeness, we discuss the main features of the solutions in the following.

The regularity of the solutions at the origin implies that $F'_0(0) = F'_1(0)$, which confirms the validity of our numerical procedures. The energy of the flat solution is $E \approx 2.376$. The pattern with two branches of solutions merging at a critical value of $\alpha_{cr} \approx 0.2333$ is also seen here [5].

The gravitating solution can be characterized by

$$E(\alpha = \alpha_{cr}) \approx 2.033, \quad A_0(\alpha = \alpha_{cr}) \approx 0.460, \quad C_m(\alpha = \alpha_{cr}) \approx 0.537. \quad (41)$$

VI. CONCLUSIONS

Our numerical results (for the three cases studied) indicate that the higher the energy of the solution is, in the flat limit, the smaller is the interval of α for which the gravitating skyrmions exist. The metric functions of the solutions on the second branch do not develop a zero in the critical limit and thus do not represent solutions with horizons. It is rather that, in this limit, the matter fields become singular at the origin. However, using a different scale for the radial variable (e.g. by reinstating the Skyrme coupling constant) would render the limiting solutions regular. Following [15], we call such solutions “gravitating sphalerons”.

Following the arguments based on Morse theory (see eg [16] and references therein), we note that the solutions on the branch with the higher energy have one more unstable mode than the solutions on the lower branch. In [5] it was argued that the solutions on the lower branches in cases I and III are stable (since the flat space limit on these branches is stable), while the solutions on the upper branch are unstable. For case II, the flat space solution on the lower branch is unstable and leads to annihilation [6]. Thus, we expect that the gravitating analogues on the lower branch are unstable and that the solutions on the upper branch have two unstable modes.

Let us mention that the situation discovered here for the cases I and III is, in many respects, similar to what happens with the electroweak skyrmion [17, 18]. In the latter case the starting theory is the standard model of electroweak interactions, in which the Higgs field plays the role of a Skyrme field and the relevant coupling constant (call it ξ) parametrizes a supplementary effective interaction (a sort of Skyrme term) encoding part of

the radiative corrections of the theory. Two branches of solutions exist which also merge at a critical value of ξ . The lower branch is stable and is the so-called “electroweak skyrmion branch” because it approaches a skyrmion solution in the limit $\xi \rightarrow 0$. The higher branch, as shown in [17], approaches either the sphaleron [15] or (according to the value of the Higgs field mass) the bisphaleron solution [19, 20].

Acknowledgements YB acknowledges the Belgian F.N.R.S. for financial support. TI thanks B Kleihaus for a useful discussion.

-
- [1] K. Lee and E.J. Weinberg, Phys. Rev. **D 44**, 3159 (1991).
 - [2] H. Luckok and I. Moss, Phys. Lett. **B 176**, 341 (1986).
 - [3] S. Droz, M. Heusler and N. Straumann, Phys. Lett. **B 268**, 371 (1988); Phys. Lett. **B 271**, 61 (1991).
 - [4] P. Bizon and T. Chmaj, Phys. Lett **B 297**, 55 (1992).
 - [5] B. Kleihaus, J. Kunz and A. Sood, Phys. Lett. **B 352**, 247 (1995).
 - [6] T. Ioannidou, B. M. A. G. Piette and W. J. Zakrzewski, J. Math. Phys. **40**, 6223 (1999); “Tbilisi 1998: Mathematical methods in modern theoretical physics” pp. 91-123 [hep-th/9811071].
 - [7] S. A. Ridgway and E. J. Weinberg, Phys. Rev. **D 52**, 3440 (1995); C. J. Houghton, N. S. Manton and P. M. Sutcliffe, Nucl. Phys. **B 510**, 507 (1998).
 - [8] N. K. Glendenning, T. Kodama and F. R. Klinkhamer, Phys. Rev. **D 38** , 3226 (1988).
 - [9] W.J. Zakrzewski, *Low dimensional sigma models* (IOP, 1989).
 - [10] A. Din and W. J. Zakrzewski, Nucl. Phys. **B 174**, 397 (1980).
 - [11] U. Ascher, J. Christiansen and R. D. Russell, Math. Comput. **33**, 658 (1979); ACM Trans. Math. Software **7**, 209 (1981).
 - [12] H. P. Künzle, Commu. Math. Phys. **162**, 371 (1994); B. Kleihaus, J. Kunz and A. Sood, Phys. Lett. **B 354**, 240 (1995).
 - [13] P. Breitenlohner, P. Forgacs and D. Maison, Nucl. Phys. **B 383**, 357 (1992); **B 442**, 126 (1995).
 - [14] A. P. Balachandran, A. Barducci, F. Lizzi, V. G. J. Rodgers and A. Stern, Phys. Rev. Lett. **52**, 887 (1984).

- [15] F. R. Klinkhamer and N. S. Manton, Phys. Rev. **D 30**, 2212 (1984).
- [16] F. V. Kusmartsev, Phys. Rep. **183**, 1 (1989).
- [17] Y. Brihaye, J. Kunz and F. Mousset, Z. Phys. **C 56**, 231 (1992).
- [18] G. Eilam, D. Klabukar and A. Stern, Phys. Rev. Lett. **56**, 1331 (1987).
- [19] J. Kunz and Y. Brihaye, Phys. Lett. **B 216**, 353 (1989).
- [20] L. G. Yaffe, Phys. Rev. **D 40**, 2723 (1989).

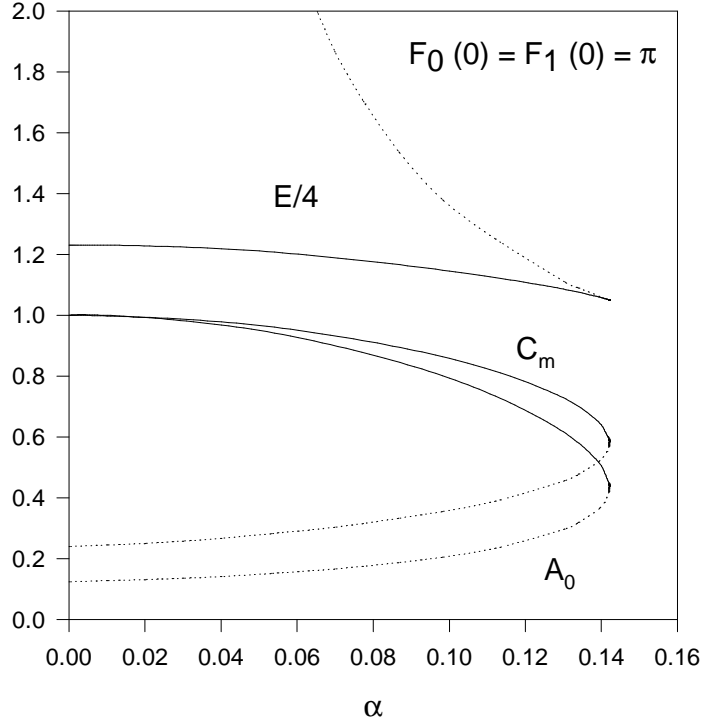


FIG. 1: The values of the metric function $A(r)$ at the origin $A(0) = A_0$, the minimal value of the metric function $C(r)$, C_m and the energy $E = \frac{4}{3\pi} \frac{m(\infty)}{\alpha^2}$ of the gravitating skyrmion solutions for case I are plotted as functions of α . The solid (respectively dotted) lines refer to the first (respectively second) branch of solutions.

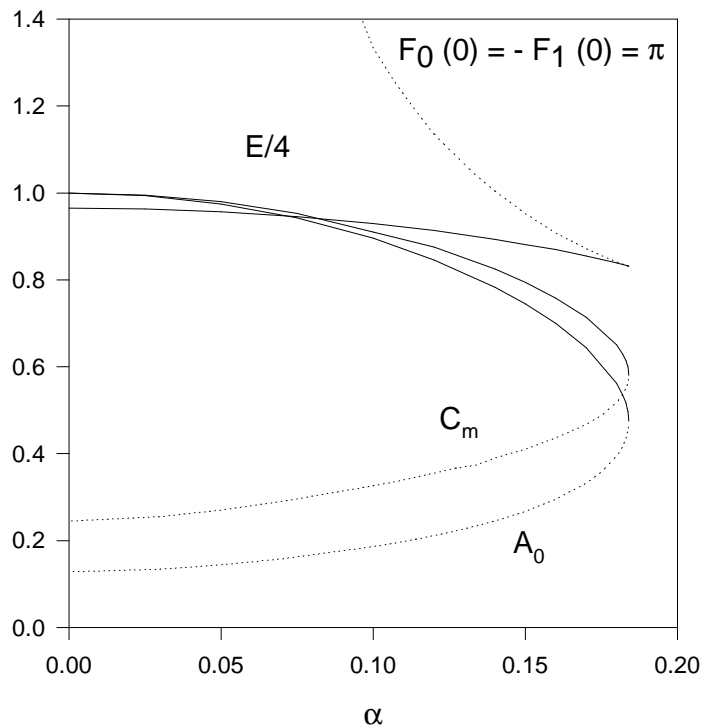


FIG. 2: The values of the metric function $A(r)$ at the origin $A(0) = A_0$, the minimal value of the metric function $C(r)$, C_m and the energy $E = \frac{4}{3\pi} \frac{m(\infty)}{\alpha^2}$ of the gravitating skyrmion solutions for case II are plotted as functions of α . The solid (respectively dotted) lines refer to the first (respectively second) branch of solutions.

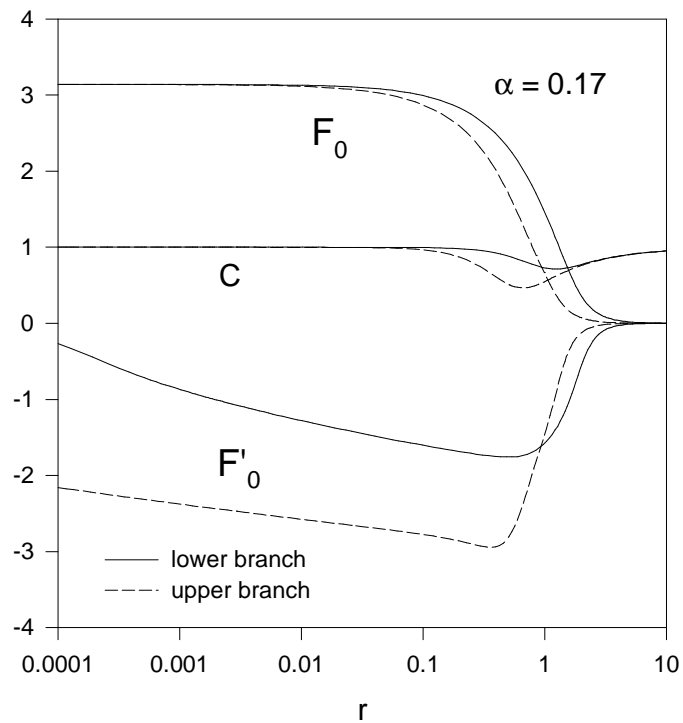


FIG. 3: The profiles of the function $F_0(r)$, $F'_0(r)$ and $C(r)$ are shown for the two branches of skyrmion-antiskyrmion solutions (case II) with $\alpha = 0.17$.